

# Time-Division Parallel FDTD Algorithm

Shinichiro Ohnuki<sup>1</sup>, Member, IEEE, Ryohei Ohnishi, Di Wu<sup>1</sup>, and Takashi Yamaguchi

**Abstract**—We propose a novel and efficient algorithm to parallelize the finite-difference time-domain method, where the observation period is divided into an arbitrary number of subsections, whose computation is distributed to corresponding computer nodes. The proposed algorithm roughly reduces the computational time to an  $n$ th fraction of the conventional algorithm, where  $n$  is the number of nodes for parallel computing, thus verifying its efficiency improvement.

**Index Terms**—Fast inverse Laplace transform, finite-difference complex-frequency-domain method, finite-difference time-domain method, time-division parallel algorithm.

## I. INTRODUCTION

WE PROPOSE a novel concept of parallelized finite-difference time-domain (FDTD) method. The resulting algorithm performs a time-division computation that roughly reduces the computational time to one  $n$ -th of the conventional algorithm, where  $n$  is the number of nodes for parallel computation. Specifically, the observation period can be divided into  $n$  subsections corresponding to the number of nodes available for computation. Then, the time-domain response can be computed for the whole observation period without requiring data exchange among nodes.

We realize this parallel algorithm using the recently developed hybrid technique that includes the finite-difference complex-frequency-domain (FDCFD) method [1] and the fast inverse Laplace transform (FILT) [2], [3], which allows to determine the initial response for each subsection. Then, the conventional FDTD method [4], [5] is applied to the initial responses to simultaneously update the electromagnetic response on all the nodes. We verify the high efficiency and accuracy of the proposed algorithm by analyzing the time-domain responses of a silver cylinder.

## II. PARALLEL FDTD ALGORITHM

Fig. 1 illustrates an example of time-division for the proposed parallel FDTD algorithm, where the observation period of  $T = 20$  fs is divided into four subsections. The calculations corresponding to the subsections are distributed to four

Manuscript received June 5, 2018; revised October 20, 2018; accepted October 30, 2018. Date of publication November 9, 2018; date of current version November 28, 2018. This work was supported in part by a Grant-in-Aid for Scientific Research (C) no. 17K06401 and in part by the Nihon University College of Science and Technology Project for Research. (*Corresponding author: Shinichiro Ohnuki*)

S. Ohnuki, R. Ohnishi, and D. Wu are with the College of Science and Technology, Nihon University, Tokyo 101-8308, Japan (e-mail: ohnuki.shinichiro@nihon-u.ac.jp; csru17008@g.nihon-u.ac.jp; cste18001@g.nihon-u.ac.jp).

T. Yamaguchi is with the Tokyo Metropolitan Industrial Technology Research Institute, Tokyo 135-0064, Japan (e-mail: yamaguchi.takashi@iri-tokyo.jp).

Digital Object Identifier 10.1109/LPT.2018.2879365

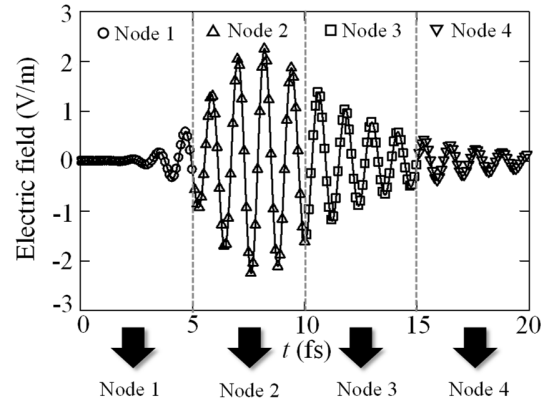


Fig. 1. Example of time-division for parallel FDTD algorithm.

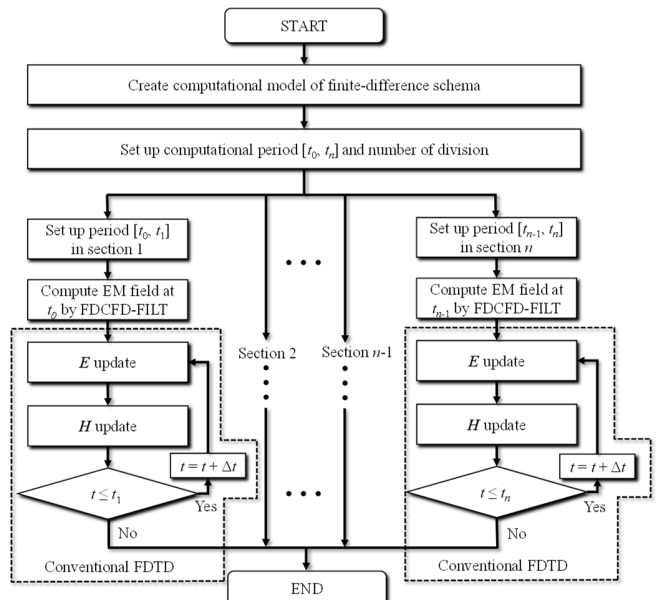


Fig. 2. Flowchart of time-division parallel FDTD algorithm. (EM: electromagnetic).

computer nodes, namely, node 1 for  $T_1 = 0\text{--}5$  fs, node 2 for  $T_2 = 5\text{--}10$  fs, node 3 for  $T_3 = 10\text{--}15$  fs, and node 4 for  $T_4 = 15\text{--}20$  fs. Each node retrieves the partial time-domain response for the allocated subsection, and hence the proposed algorithm does not require data exchange among the nodes during the parallel computation.

Fig. 2 shows the flowchart of the proposed algorithm that consists of five steps:

- 1) Establish a computational model using the conventional FDTD method, where model data are shared among nodes.

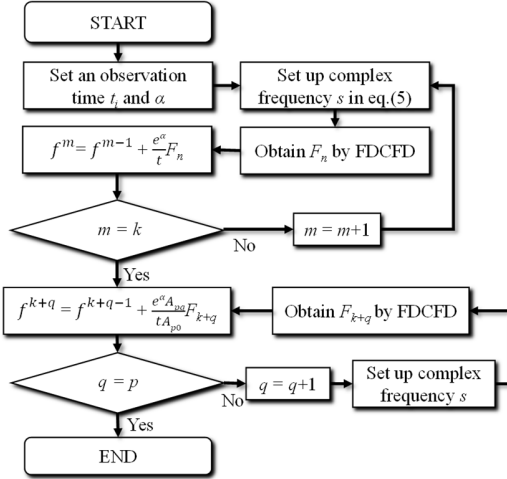


Fig. 3. Flowchart of the initial response calculation of a subsection by FDCFD–FILT at observation time  $t$ .

2) Divide the observation period,  $T = t_0 - t_n$ , into  $n$  subsections:  $T_1 = t_0 - t_1$ ,  $T_2 = t_1 - t_2, \dots, T_n = t_{(n-1)} - t_n$ .

3) Compute the initial response of electromagnetic field at  $t_0, t_1, \dots, t_{n-1}$  on the corresponding  $n$  nodes. This step allows to realize the parallel algorithm as detailed below.

4) Using the initial values obtained in step 3, the conventional FDTD method is simultaneously applied on all the nodes to update the electromagnetic field estimates in the subsections. This process is completely parallel as no data exchange occurs among nodes.

5) The complete response for the observation period is obtained by merging the partial responses of all the subsections.

Besides step 3, the proposed parallel algorithm is simple as it only applies the conventional FDTD method. The process to obtain the initial responses at instants  $t_0, t_1, \dots$ , and  $t_{n-1}$  in step 3 is based on the hybrid FDCFD–FILT technique [1], depicted in Fig. 3 and detailed as follows:

i) We use an FDCFD formula that derives from the finite-difference frequency-domain method [6]–[8]. The time dependence of the Maxwell's equations is assumed to be  $e^{st}$ , where the complex frequency is represented by  $s = \sigma + j\omega$ . The following finite-difference form can be obtained by replacing the partial derivative with respect to time by the two-dimensional TE case:

$$\frac{H_z(i + 0.5, j + 0.5) - H_z(i + 0.5, j - 0.5)}{\Delta y} - s\epsilon_0\epsilon_r E_x(i + 0.5, j) = J_x(i + 0.5, j), \quad (1)$$

$$\frac{H_z(i - 0.5, j + 0.5) - H_z(i + 0.5, j + 0.5)}{\Delta x} - s\epsilon_0\epsilon_r E_y(i, j + 0.5) = J_y(i, j + 0.5), \quad (2)$$

$$\frac{E_x(i + 0.5, j) - E_x(i + 0.5, j + 1)}{\Delta y} + s\mu_0\mu_r H_{zy}(i + 0.5, j + 0.5) = 0, \quad (3)$$

$$\frac{E_y(i + 1, j + 0.5) - E_y(i, j + 0.5)}{\Delta x} + s\mu_0\mu_r H_{zx}(i + 0.5, j + 0.5) = 0, \quad (4)$$

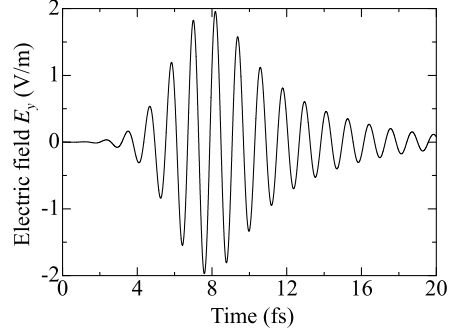


Fig. 4. Modulated Gaussian pulse incidence obtained from conventional FDTD method.

where  $i$  and  $j$  are the coordinates of the lattice points in the  $x$  and  $y$  directions, respectively,  $\Delta x$  and  $\Delta y$  determine the size of a unit cell, and  $H_{zx}$  and  $H_{zy}$  are the components of  $H_z$  propagating along the  $x$  and  $y$  directions, respectively. Then, the simultaneous equations for computing the electromagnetic field can be obtained by applying the abovementioned equations over the entire computational space, where the unknown electromagnetic field components in the complex-frequency domain can be evaluated using either a direct or an iterative solver [9].

ii) After determining the electromagnetic fields in the complex-frequency domain, the time-domain response at  $t_i$  ( $i = 0, 1, \dots, n - 1$ ) can be obtained using the FILT. Response  $f$  can be computed to evaluate the following finite series [2], [3]:

$$f(t_i) = \frac{e^{\alpha}}{t} \left( \sum_{m=1}^k F_m + \frac{1}{A_{p0}} \sum_{q=1}^p A_{pq} F_{k+q} \right), \quad (5)$$

where

$$F_m = (-1)^m \operatorname{Im}[F(s)], s = \frac{\alpha + j(m - 0.5)\pi}{t_i}, \quad (6)$$

$$A_{pp} = 1, A_{p0} = 2^p, A_{pq} = A_{pq-1} - \frac{(p+1)!}{q!(p+1-q)!}, \quad (7)$$

$F(s)$  is the image function,  $\alpha$  is the approximation parameter determining the accuracy,  $k$  is the truncation number, and  $p$  is another truncation number for executing the Euler transformation [1]. This process can be completely parallelized over  $n$  nodes.

iii) The conventional FDTD method is applied on the obtained the initial response  $f(t_i)$ , and the electromagnetic response can be updated as detailed in Fig. 2.

### III. COMPUTATIONAL RESULTS

We verified the performance and accuracy of the proposed parallel FDTD algorithm using modulated Gaussian pulse incidence on a two-dimensional silver cylinder with diameter  $d = 1$  nm and the time-domain response obtained by the conventional FDTD method [4], [5] shown in Fig. 4. The electric field is evaluated at 0.1 nm along the lateral direction away from the surface of cylinder. The center wavelength of the Gaussian pulse was set to 350 nm for exciting the surface

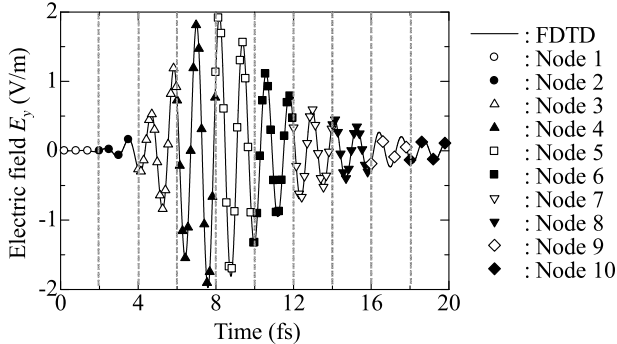


Fig. 5. Modulated Gaussian pulse incidence obtained from proposed time-division parallel FDTD algorithm.

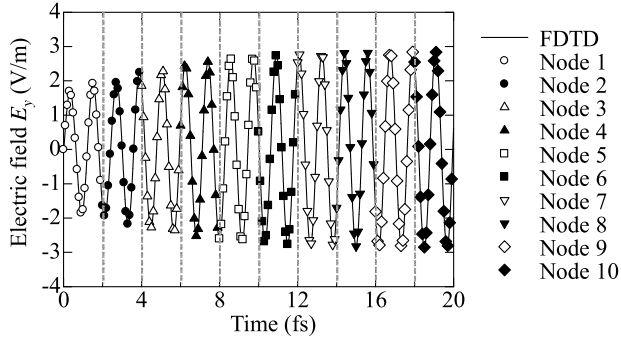


Fig. 6. Result of continuous plane wave incidence using time-division parallel FDTD algorithm.

plasmon at bandwidth of 84 nm. To model the cylinder using a square cell of size  $\Delta x = \Delta y = 0.01$  nm, we evaluated the electromagnetic field over observation period  $T = 0\text{--}20$  fs with timestep  $\Delta t = 2 \times 10^{-5}$  fs to satisfy the CFL condition. The frequency dispersion of the permittivity in the complex-frequency domain was assumed to follow the Lorentz–Drude model:

$$\epsilon_r(s) = 1 + \frac{f_0\omega_p^2}{s^2 + s\Gamma_0} + \sum_{j=1}^N \frac{f_j\omega_p^2}{s^2 + s\Gamma_j + \omega_j^2}, \quad (8)$$

where  $\omega_p$  is the plasma frequency and  $N$  is the number of oscillators at frequency  $\omega_j$ , strength  $f_j$ , and damping coefficient  $\Gamma_j$ . These parameters were selected as in [10].

We applied the proposed parallel FDTD algorithm using time division to compare it with the conventional algorithm. The observation period was divided into 10 subsections and the computational tasks were equally distributed to 10 nodes with the same characteristics. Hence, each subsection contained 2 fs of data points. The time-domain response obtained using the proposed algorithm is shown in Fig. 5 and suitably agrees with that obtained using the conventional FDTD method.

We conducted a similar simulation for continuous wave incidence with wavelength of 350 nm. The transient response shown in Fig. 6 was obtained using the proposed time-division parallel algorithm and is in excellent agreement with that using the conventional FDTD method. Note that the field intensity is gradually enhanced due to plasmonic resonance. In addition, we investigated the computational accuracy for the initial response at  $t_5 = 10$  fs. Fig. 7 shows the convergence

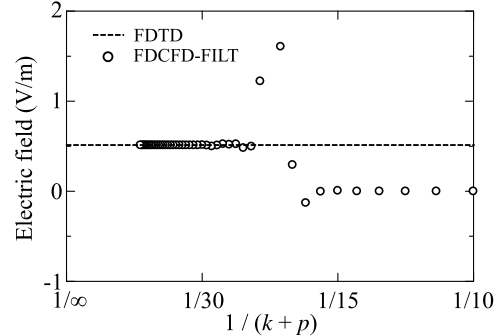


Fig. 7. Accuracy of FDCFD–FILT technique according to truncation number  $k$  at  $t = 10$  fs considering approximation parameter  $\alpha = 5$  and truncation number for Euler transformation  $p = 3$ .

TABLE I  
COMPARISON OF INITIAL RESPONSES USING CONVENTIONAL  
FDTD AND FDCFD–FILT TECHNIQUE

Observation time (fs)	Conventional FDTD (V/m)	FDCFD–FILT (V/m)
2	-1.63296	-1.63310
4	1.86211	1.86186
6	0.70091	0.70106
8	-2.60059	-2.60077
10	0.51115	0.51102
12	2.53551	2.53611
14	-1.70954	-1.70926
16	-1.80501	-1.80539
18	2.55140	2.55108

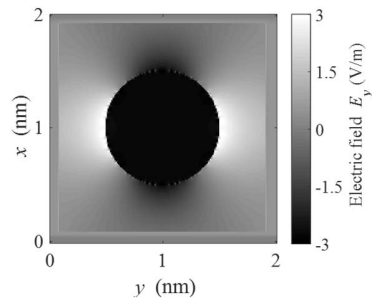


Fig. 8. Distribution of electric field component  $E_y$  at  $t = 18$  fs obtained from time-division parallel FDTD algorithm.

according to truncation number  $k$  of the FDCFD–FILT technique to obtain the initial response with approximation parameter  $\alpha = 5$  and truncation number for Euler transformation  $p = 3$ . The value converges to the original FDTD result up to four decimals of precision when  $k \geq 30$ . The initial responses for all the subsections are listed in Table I, which confirms the agreement between the conventional FDTD result and the FDCFD–FILT technique up to four decimals. Fig. 8 shows the distribution of electric field  $E_y$  at  $t = 18$  fs obtained from the time-division FDTD algorithm. The surface plasmon is excited by incidence, and the field intensity enhanced. The normalized relative error between the time-division algorithm and conventional FDTD method is shown in Fig. 9, exhibiting an error below 0.01% throughout the computational space.

Finally, we evaluated the computational time of the proposed algorithm. The computational time for the conventional

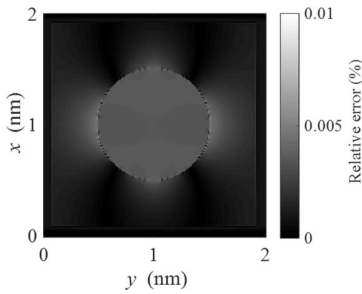


Fig. 9. Normalized relative error between time-division parallel algorithm and conventional FDTD.

TABLE II  
COMPUTATIONAL TIME OF PARALLEL FDTD ALGORITHM  
AT DIFFERENT PERIODS

Observation period (fs)	CPU time of FDTD (s)	CPU time of initial response (s)	Total time (s)
0–2	578.69	—	578.69
2–4	579.26	62.66	641.92
4–6	577.91	66.58	644.49
6–8	575.95	75.17	651.12
8–10	577.54	82.59	660.13
10–12	578.27	89.82	668.09
12–14	579.16	103.55	682.71
14–16	572.95	109.88	682.83
16–18	576.22	100.53	676.75
18–20	575.02	105.56	680.75
0–20	5835.78	—	5835.78

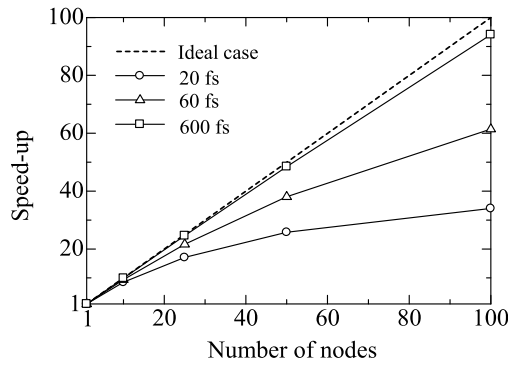


Fig. 10. Speed-up of parallel FDTD algorithm according to the number of nodes.

single-node FDTD calculation is approximately 6000 s. As shown in Table II, the proposed parallel algorithm retrieves computational times of approximately 600 s for the FDTD method and 100 s for determining the initial responses using the FDCFD–FILT technique per node.

Fig. 10 depicts the speed-up of the time-division parallel FDTD algorithm when varying the number of nodes [11]. When the computation nodes increase from 1 to 100, the speed-up increases. For the observation time of 600 fs, it follows the ideal case and reaches over 94 for 100 nodes. It tends to be saturated around 25 nodes for the observation time of 20 fs, since the computational cost of obtaining the

initial response becomes more expensive than that for FDTD computation. In our proposed algorithm, the time for FDTD computation is always reduced to an  $n$ -th fraction, where  $n$  is the number of nodes. On the other hand, the time to obtain the initial response remains almost constant. Extrapolating to an infinite number of nodes, the CPU time to compute the FDTD would be zero for a constant initial response time. In our future work, the optimized selection of the number of nodes and observation period will be investigated.

#### IV. CONCLUSION

We propose a simple and efficient algorithm for time-division parallel FDTD algorithm. The proposed algorithm allows to divide the observation period into an arbitrary number of subsections, whose calculations are distributed to corresponding computer nodes. Moreover, the algorithm is completely parallel, because no data exchange among nodes occurs during computation. The proposed algorithm can be highly efficient to study a wide variety of time-domain electromagnetic, optic, and plasmonic problems, as it notably reduces the computational time.

#### REFERENCES

- [1] D. Wu, R. Ohnishi, R. Uemura, T. Yamaguchi, and S. Ohnuki, “Finite-difference complex-frequency-domain method for optical and plasmonic analyses,” *IEEE Photon. Technol. Lett.*, vol. 30, no. 11, pp. 1024–1027, Jun. 1, 2018, doi: [10.1109/LPT.2018.2828167](https://doi.org/10.1109/LPT.2018.2828167).
- [2] T. Hosono, “Numerical inversion of Laplace transform and some applications to wave optics,” *Radio Sci.*, vol. 16, no. 6, pp. 1015–1019, Nov./Dec. 1981, doi: [10.1029/RS016i006p01015](https://doi.org/10.1029/RS016i006p01015).
- [3] S. Kishimoto, T. Okada, S. Ohnuki, Y. Ashizawa, and K. Nakagawa, “Efficient analysis of electromagnetic fields for designing nanoscale antennas by using a boundary integral equation method with fast inverse Laplace transform,” *Prog. Electromagn. Res.*, vol. 146, pp. 155–165, 2014, doi: [10.2528/PIER13081701](https://doi.org/10.2528/PIER13081701).
- [4] K. Yee, “Numerical solution of initial boundary value problems involving Maxwell’s equations in isotropic media,” *IEEE Trans. Antennas Propag.*, vol. TAP-14, no. 3, pp. 302–307, May 1966, doi: [10.1109/TAP.1966.1138693](https://doi.org/10.1109/TAP.1966.1138693).
- [5] A. Taflove and S. C. Hagness, *Computational Electrodynamics: The Finite-Difference Time-Domain Method*, 2nd ed. Norwood, MA, USA: Artech House, 2000.
- [6] V. Varadarajan and R. Mittra, “Finite-difference time-domain (FDTD) analysis using distributed computing,” *IEEE Microw. Guided Wave Lett.*, vol. 4, no. 5, pp. 144–145, May 1994, doi: [10.1109/75.289515](https://doi.org/10.1109/75.289515).
- [7] E. I. Wei, W. C. H. Choy, and W. C. Chew, “A comprehensive study for the plasmonic thin-film solar cell with periodic structure,” *Opt. Express*, vol. 18, no. 6, pp. 5993–6007, 2010, doi: [10.1364/OE.18.005993](https://doi.org/10.1364/OE.18.005993).
- [8] F. Xu, Y. Zhang, W. Hong, K. Wu, and T. J. Cui, “Finite-difference frequency-domain algorithm for modeling guided-wave properties of substrate integrated waveguide,” *IEEE Trans. Microw. Theory Techn.*, vol. 51, no. 11, pp. 2221–2227, Nov. 2003, doi: [10.1109/TMTT.2003.818935](https://doi.org/10.1109/TMTT.2003.818935).
- [9] W. H. Press, S. A. Teukolsky, W. T. Vetterling, and B. P. Flannery, *Numerical Recipes in C*, 2nd ed. New York, NY, USA: Cambridge Univ. Press, 1992.
- [10] A. D. Rakic, A. B. Djurić, J. M. Elazar, and M. L. Majewski, “Optical properties of metallic films for vertical-cavity optoelectronic devices,” *Appl. Opt.*, vol. 37, no. 22, pp. 5271–5283, Aug. 1998, doi: [10.1364/AO.37.005271](https://doi.org/10.1364/AO.37.005271).
- [11] A. C. Lesina, A. Vaccari, P. Berini, and L. Ramunno, “On the convergence and accuracy of the FDTD method for nanoplasmatics,” *Opt. Express*, vol. 23, no. 8, pp. 10481–10497, 2015, doi: [10.1364/OE.23.010481](https://doi.org/10.1364/OE.23.010481).